ACTA TEHNICA CORVINIENSIS – Bulletin of Engineering
Tome VIII [2015] Fascicule 3 [July – September]
ISSN: 2067 – 3809

[1.] Diana Alina BISTRIAN, [2.] Romeo F. SUSAN-RESIGA

CHARACTERIZATION OF SWIRLING FLOW AT INLET OF HYDRAULIC TURBINES DRAFT CONE BY PROPER ORTHOGONAL DECOMPOSITION

[1.] Department of Electrical Engineering and Industrial Informatics, "Politehnica" University of Timişoara, Revolutiei 5, Hunedoara, ROMANIA,
[2.] Department of Hydraulic Machinery, "Politehnica" University of Timişoara, Bvd. Mihai Viteazu 1, Timisoara, ROMANIA

Abstract: *In this paper we employ the method of proper orthogonal decomposition (POD) in conjunction with the radial basis functions interpolation (RBF) for characterization of the swirling flow at the inlet of the draft cone of hydraulic turbines by modal decomposition. The efficiency of the reduced order model is tested by employing different kernels for RBF interpolation and a rigorous error analysis for the obtained reduced order model is performed.*
Keywords: *proper orthogonal decomposition, hydraulic turbines, reduced order modeling*

INTRODUCTION

The increased quantity of information in parameter dependent problems necessitate simulation algorithms and complex data processing, whose efficiency depends on the degree of accuracy and time required to obtain useful information. The modeling of self-induced instabilities in turbomachinery depending on the discharge coefficient [1], investigations on dynamic stall control with passive elements [2] or magnetic interactions between the nanoparticles [3] are some pertinent examples.

The problem investigated in this paper originates from turbomachinery, where the direct application of model order reduction concepts for fluid control is not straightforward, mainly because of the nonlinearity of the Navier-Stokes equations. Our focus is to provide a solution to obtain a reduced model which accurately represents dominant features of the flow at the inlet of the draft cone.

In this paper we employ a data driven method of Proper Orthogonal Decomposition (POD), that use sample stored experimental data to generate the spatial modes. The POD method was introduced by several scientists independently, for different applications, in particular by Kosambi [4], Loeve [5], Karhunen [6] and Obukhov [7] and has been illustrated on a variety of examples ranging from fluid mechanics [8], turbulent flows [9] and oceanography [10].

The remainder of this article is organized as follows. The procedure of numerical data acquisition is presented in Section 2. The principles governing the Proper Orthogonal Decomposition are discussed in detail in Section 3 that includes also an algorithm for computing the proper orthogonal modes. We devote the Section 4 to reveal the numerical results estimated for the hydraulic turbine within the full operating range. The results are compared to an existing measurement for radial velocity profiles. Summary and conclusions are drawn in the final section.

NUMERICAL DATA ACQUISITION

Francis turbines cover the largest part of the installed hydropower capacity in the world, owing their name to the British-American engineer James B. Francis in the 1840s. A cross-section of the device is presented in Figure 1. The flow enters through a volute or scroll casing which is designated to evenly distribute the flow around the periphery of the inlet guide vanes. As the inlet guide vanes increase the angular momentum of the fluid, the turbine rotor turns the flow from the radial to the axial direction. The draft cone is the machine component where the flow exiting the runner is decelerated, where the excess of kinetic energy is converted into static pressure.

In order to derive the mathematical model of the swirling flow in the draft cone, we express the physical quantities in their dimensionless form using a reference radius R_{ref} *chosen as the runner outlet radius and a reference velocity* $V_{ref} = \Omega R_{ref}$, *where* Ω *represents the runner angular velocity. In consequence, by introducing the dimensionless velocity* $v = V / \left(\Omega R_{ref}\right)$ *we are concerned on the axial-tangential velocity profile* $\left(v_z, v_\theta\right)$ *downstream the runner, corresponding to the radial section* $S = \left\{ r \,\middle|\, r \in \left[0, r_w\right] \right\}$, *where* $r_w = R_w / R_{ref}$ *is the dimensionless radial distance to the cone wall and has the value* 1.063 *in our test bench (see Figure 1).*

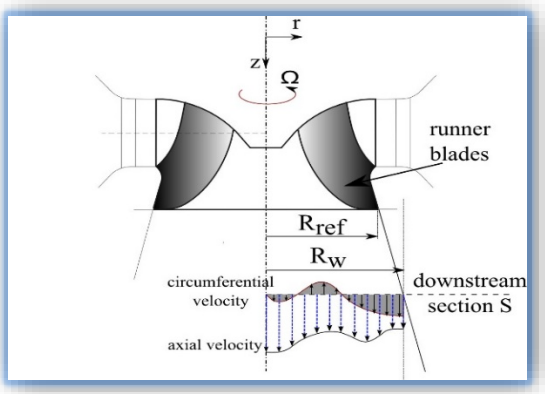

Figure 1. Meridional cross-section of the draft cone

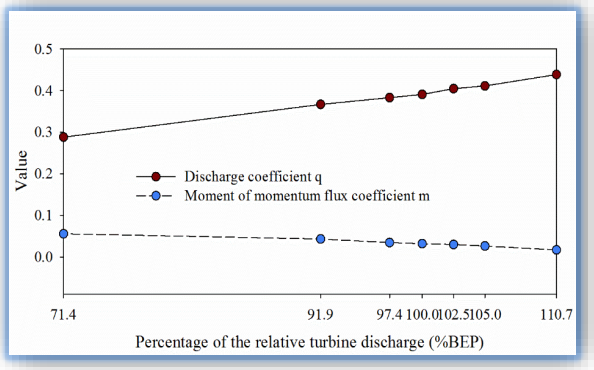

Figure 2. The two main integral parameters that characterize the swirling flow in the section S at each operating point

A turbine operating regime is defined by the pair (q,m) *where the turbine discharge* q *and the flux of moment of momentum* m *are evaluated in dimensionless form as*

$$q=\int_0^{r_w} v_z 2rdr,\quad m=\int_0^{r_w}(rv_\theta)v_z 2rdr. \tag{1}$$

The integrals in relations (1) are computed using the Simpson $1/3$ *rule and the corresponding values are given in Figure 2.*

First we consider the velocities expressed as a juxtaposition of a basic flow $(v_z{}^0, v_\theta{}^0)$ *and a perturbation part* $(\hat{v}_z,\hat{v}_\theta)$ *such that such that all the operating regimes exhibit a null discharge coefficient of the axial fluctuation and also a null flux of moment of momentum of the circumferential fluctuation. According to definitions (1), this is mathematically achieved by writing*

$$v_z=v_z{}^0+\hat{v}_z,\quad \int_0^{r_w}\hat{v}_z 2rdr=0, \tag{2}$$

$$v_\theta=v_\theta{}^0+\hat{v}_\theta,\quad \int_0^{r_w}(r\hat{v}_\theta)v_z 2rdr=0. \tag{3}$$

Next we compute the velocity components of the base flow such that the conditions (2) and (3) hold. It follows from (1) that

$$q=\int_0^{r_w} v_z{}^0 2rdr+\int_0^{r_w}\hat{v}_z 2rdr \tag{4}$$

and considering (2) yields that the axial velocity of the base flow is

$$v_z{}^0=\frac{q}{r_w{}^2}. \tag{5}$$

Considering that the fluctuation part of the circumferential velocity is expressed as product between the radial coordinate and the angular velocity $v_\theta{}^0=\omega^0 r$*, it follows from (1) that*

$$m=\int_0^{r_w}(\omega^0 r^2)v_z 2rdr+\int_0^{r_w}(r\hat{v}_\theta)v_z 2rdr \tag{6}$$

and considering (3) yields the expression of the circumferential velocity of the base flow as

$$v_\theta{}^0=\omega^0 r,\ \ \omega^0=m\left(2\int_0^{r_w} v_z r^3 dr\right)^{-1}. \tag{7}$$

In order to derive the mathematical model of the velocity components, we consider seven operating regimes covering both the overload, the best efficiency point (BEP) and the partial load behavior of Francis turbine. Both axial and circumferential velocity profiles are measured in the survey section S *downstream the runner, using Laser Dopler Velocimetry technique [11]. These measurements are used to develop the reduced order model that predicts the inlet velocity components for the operating regimes for which the experimental measurement are not available. We will further detail the results in the section dedicated to numerical experiments.*

POD-RBF ALGORITHM FOR REDUCED ORDER MODELING

We concentrate in this section to approximate the velocity components of the swirling flow fluctuation $\hat{v}=(\hat{v}_z,\hat{v}_\theta)$ *as a finite sum of form*

$$\hat{v}(r)\approx\sum_{j=1}^{p} a_j\phi_j(r). \tag{8}$$

In Proper Orthogonal Decomposition approach, we seek for an orthonormal basis functions, i.e.

$$\langle\phi_i(r),\phi_j(r)\rangle_{L^2(S)}=\delta_{ij}, \tag{9}$$

where δ_{ij} *is the Kronecker delta symbol and the coefficients* $a_j, j=1,\dots,p$ *are computed by projecting the velocity field onto the POD modes*

$$a_j=\langle\hat{v}(r),\phi_j(r)\rangle_{L^2(S)}. \tag{10}$$

This leads to the following POD algorithm for identification of the velocity field in the draft tube of hydraulic turbine, based on the singular value decomposition (SVD):

(i) Collect data $v(r_i;q_\ell)$, $i=1,\dots,m$, $\ell=1,\dots,N$ *at survey section* S *for* N *operating regimes.*

(ii) Arrange the set of data in an $m\times N$ *matrix called the snapshot data matrix,*

$$A=\begin{pmatrix} v(r_1;q_1) & v(r_1;q_2) & \dots & v(r_1;q_{N-1}) & v(r_1;q_N)\\ v(r_2;q_1) & v(r_2;q_2) & \dots & v(r_2;q_{N-1}) & v(r_2;q_N)\\ \vdots & \vdots & \vdots & \vdots & \vdots\\ v(r_m;q_1) & v(r_m;q_2) & \dots & v(r_m;q_{N-1}) & v(r_m;q_N)\end{pmatrix}.$$

(iii) Compute the base flow matrix B^0 *in the following form:*

$$B^0 \equiv B_z^0 = \left[q_1 / r_w^2 \quad q_2 / r_w^2 \quad \dots \quad q_N / r_w^2 \right]$$

$$for\ v(r;q) \equiv v_z(r),$$

$$B^0 \equiv B_\theta^0 = \begin{pmatrix} r_1\omega_1^0 & r_1\omega_2^0 & \dots & r_1\omega_{N-1}^0 & r_1\omega_N^0 \\ r_2\omega_1^0 & r_2\omega_2^0 & \dots & r_2\omega_{N-1}^0 & r_2\omega_N^0 \\ \vdots & \vdots & \vdots & \vdots & \vdots \\ r_m\omega_1^0 & r_m\omega_2^0 & \dots & r_m\omega_{N-1}^0 & r_m\omega_N^0 \end{pmatrix} \in \mathbb{R}^{m\times N}$$

$$for\ v(r;q) \equiv v_\theta(r).$$

(iv) Compute the base flow-subtracted snapshot matrix $\mathcal{A} = A - B^0$.

(v) We employ an economy size singular value decomposition (SVD) of $\mathcal{A}$ *that guarantees the existence of real numbers* $\lambda_1 \ge \lambda_2 \ge \dots \ge \lambda_d > 0$ *and orthogonal matrices* $\Phi \in \mathbb{R}^{m\times m}$ *and* $\Psi \in \mathbb{R}^{N\times N}$ *such that* $\mathcal{A} = \Phi D \Psi^T$, *where* $D = diag(\lambda_1,\dots,\lambda_d) \in \mathbb{R}^{d\times d}$.

(vi) The column space of $\mathcal{A}$ *can be represented in terms of the* d *linearly independent columns of* Φ . *Since* Φ *is orthogonal, we find that the columns of the snapshot matrix* $\mathcal{A}$ *are*

$$v_\ell = \sum_{i=1}^{d} \mathcal{A}_{i\ell}\Phi_{:,i} = \sum_{i=1}^{d} \left(D(\Psi)^T \right)_{i\ell} \phi_i =$$

$$= \sum_{i=1}^{d} \left(\underbrace{(\Phi)^T \Phi}_{I_d} D(\Psi)^T \right)_{i\ell} \phi_i = \sum_{i=1}^{d} \left((\Phi)^T \mathcal{A} \right)_{i\ell} \phi_i =$$

$$= \sum_{i=1}^{d} \left(\underbrace{\sum_{k=1}^{N} \Phi_{ki} \mathcal{A}_{k\ell}}_{=\phi_i^T v_\ell} \right) \phi_i = \sum_{i=1}^{d} \langle \phi_i, \mathrm{v}_\ell \rangle_{\mathbb{R}^m} \phi_i ,$$

where $I_d \in \mathbb{R}^{d\times d}$ *stands for the identity matrix and* $\langle \cdot,\cdot \rangle_{\mathbb{R}^m}$ *denotes the canonical inner product in* $\mathbb{R}^m$.

One measure of the effectiveness of POD is related to the rate of decay of the eigenvalues. We define the relative energy content (REC) of the singular value decomposition of $\mathcal{A}$ *by*

$$REC_{POD}(p) = \frac{\sum_{j=1}^{p} \lambda_j}{\sum_{j=1}^{d} \lambda_j} \qquad (11)$$

Table 1. Kernels for RBF interpolation

Name of the Kernel	Definition
Cubic	$k(z) = z^3$
Gaussian	$k(z) = \exp\left(-\frac{z^2}{2\sigma^2}\right)$
Thinplate	$k(z) = r^2 \ln(z+1)$
Multiquadric	$k(z) = \sqrt{1+\frac{z^2}{\sigma^2}}$

and we find the number of POD basis vectors $p < d$ *when the low-rank approximation is required to contain* $\delta\%$ *of the total information contained in the original snapshot matrix. The dimension of the subspace spanned by the first* p *singular modes* $\{\phi_j\}_{j=1}^{p}$ *is determined by*

$$p = \arg\min\{REC_{POD}(p); REC_{POD}(p) \ge \delta\}. \qquad (12)$$

Usually, we consider $99.00\% \le \delta \le 99.99\%$ *and by employing the radial basis function (RBF) interpolation, the coefficients* $a_j, j = 1,\dots,p$ *of the reduced order model can be determined for any operating regime* q .

Considering the precomputed POD coefficients as a set of distinct nodes $\{\mathbf{x}_i\}_{i=1}^{p\times N} \subset \mathbb{R}^2$ *and a set of function values* $\{f_i\}_{i=1}^{p\times N} \subset \mathbb{R}$, *the problem reduces to find an interpolant* $s : \mathbb{R}^2 \to \mathbb{R}$ *such that*

$$s(\mathbf{x}_i) = f_i \quad for\ i = 1,\dots,p\times N, \qquad (13)$$

where N *is the number of operating regimes for which experimentally measured data are available and* p *is the number of POD modes provided by the energy criterion (11). Note that we use the notation* $\mathbf{x} = (x,y) \in \{1,\dots,p\} \times [q_1, q_N]$ *for scattered points coordinates and* $f_i = a_j^\ell$, $\mathrm{j} = 1,\dots,\mathrm{p}$, $\ell = 1,\dots,N$ *for scattered points values. Following Duchon [13], the solution to the problem (12) is a function of the form*

$$s(\mathbf{x}) = \sum_{i=1}^{p\times N} w_i k\left(\|\mathbf{x} - \mathbf{x}_i\|_2\right) + \mathrm{P}(\mathbf{x}), \qquad (14)$$

where k *is a real valued function defined on the kernel* $k \in K : \mathbb{R}^{p\times N} \times \mathbb{R}^{p\times N} \to \mathbb{R}$, $\|\cdot\|_2$ *is the Euclidian distance between the points* $\mathbf{x}$ *and* $\mathbf{x}_i$, *the coefficients* $w_i \in \mathbb{R}$ *are constant real numbers, while* $\mathrm{P}(x)$ *is a global polynomial function of total degree at most* $n-1$ *with* n *considered small. The points* $\mathbf{x}_i$ *are referred as centers of the Radial Basis Functions* $k(z) = K(\mathbf{x}, \mathbf{x}_i)$, *where the variable* z *stands for* $\|\mathbf{x} - \mathbf{x}_i\|_2$.

Table 1 lists the kernels for RBFs that we use in the following experiments, where parameter σ *is the shape parameter of the RBF. Changing the shape parameter of an RBF alters the interpolant surface, thus can have a significant impact on the accuracy of the approximation. Finding the shape parameter that will produce the most accurate approximation is a topic of current research. Investigations upon accuracy and stability of RBF based interpolation may be found in Fornberg and Wright [14].*

Considering that $\{p_1, p_2, \dots, p_n\}$ *represents a basis for the polynomial* $\mathrm{P}(\mathbf{x})$ *and* $\{c_1,\dots,c_n\}$ *are the coefficients that give the polynomial* $\mathrm{P}(\mathbf{x})$ *in terms of this basis, introducing Eq. (14) into (13) leads to a linear system to be solved for the coefficients that specify the RBF.*

The methodology presented herein leads to the following POD-RBF linear model for estimation of the perturbation part of the velocity field for the entire operating range.

$$\hat{v}(r;q) = \sum_{j=1}^{p} a_j^q \phi_j(r), \quad a_j^q = s(x,y),$$

$$x = j \in \{1,\ldots,p\},\ y = q \in [q_1, q_N], \qquad (15)$$

where a_j^q are the interpolated POD coefficients, $\phi_j(r)$ are the POD basis functions, p represents the number of the POD basis functions retained for the low order model and q denotes the value of the discharge coefficient.

VALIDATION OF POD-RBF MODEL AND NUMERICAL RESULTS

The aim of this section is twofold: first we verify the accuracy of the POD-RBF low order model developed herein and second, we illustrate the computational efficiency of the proposed model by employing different kernels for RBF interpolation.

Considering the set of $N = 7$ experimentally measured profiles representing the axial and circumferential velocities at the inlet of the draft tube (see Figure 1), experimentally measured for discharge coefficients settled in Figure 2, we employ the POD algorithm described in Section 3 to obtain a reduced order model of the velocity fields. The logarithmic plots of the singular values obtained from POD decomposition of the axial velocity perturbation and circumferential velocity perturbation are presented in Figure 3a and Figure 4a, respectively.

The relative energy content captured as the number of the POD modes is presented in Figure 3b and Figure 4b, respectively, for both velocity fields. Most of the energy defined by Equation (11) is contained in the first few modes.

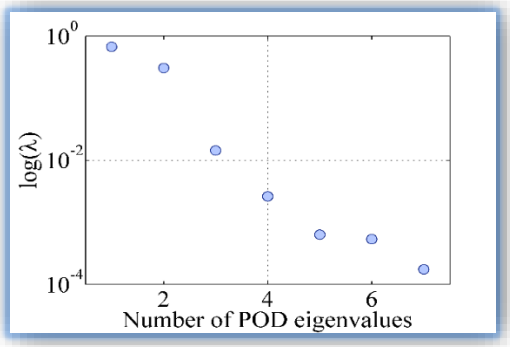

a.

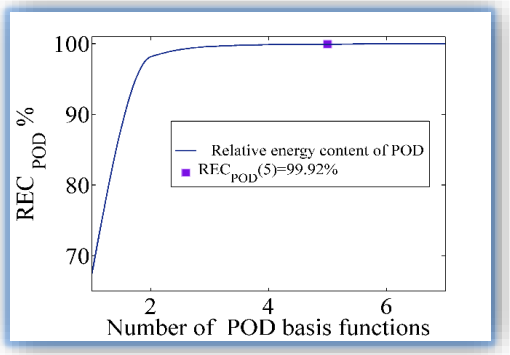

b.

Figure 3. a. POD eigenvalues of the axial velocity decomposition; b. Relative energy content captured by POD decomposition as the number of the POD modes

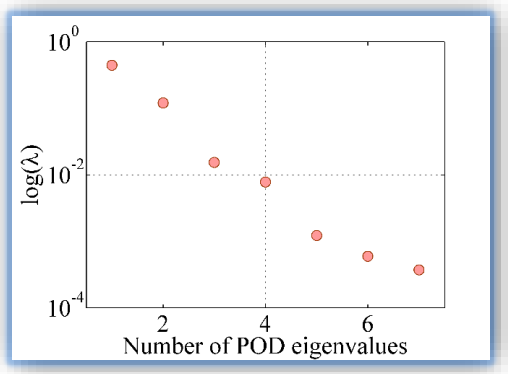

a.

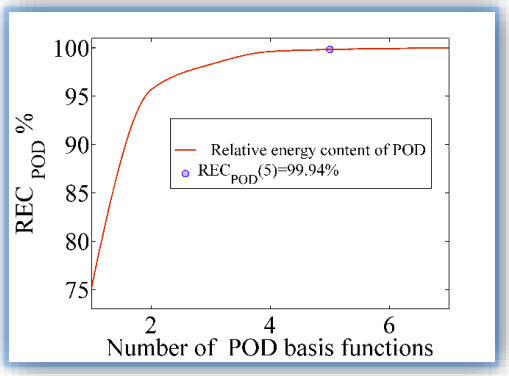

b.

Figure 4. a. POD eigenvalues of the circumferential velocity decomposition; b. Relative energy content captured by POD decomposition as the number of the POD mode

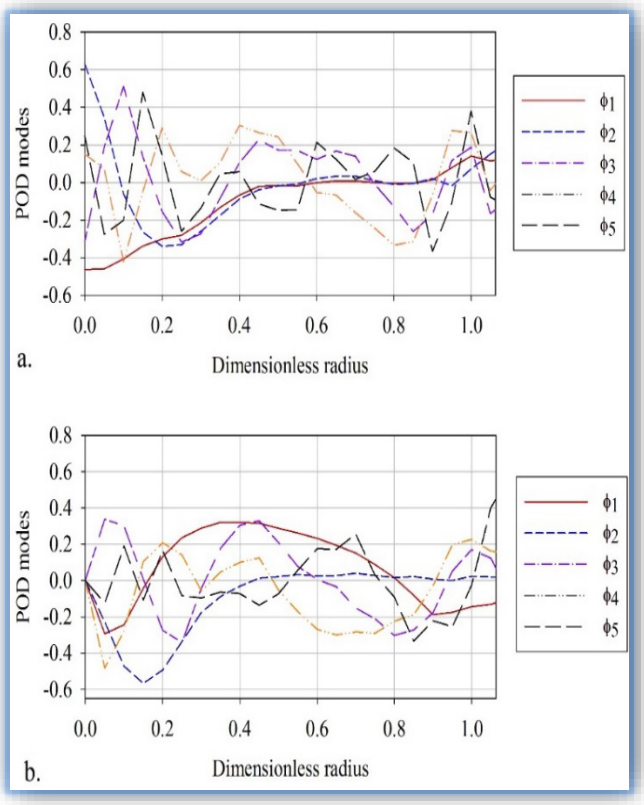

Figure 5. POD basis functions of the axial velocity decomposition (a) and circumferential velocity decomposition (b).

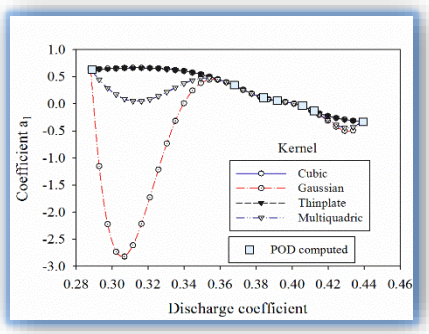

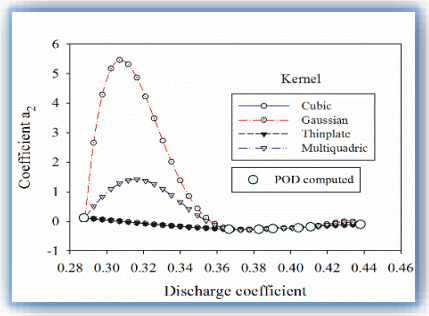

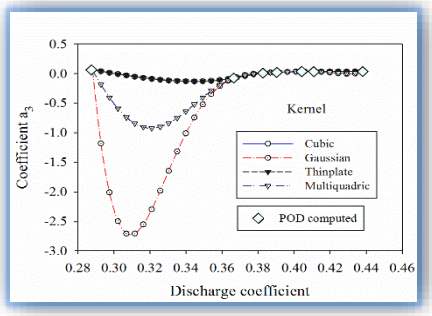

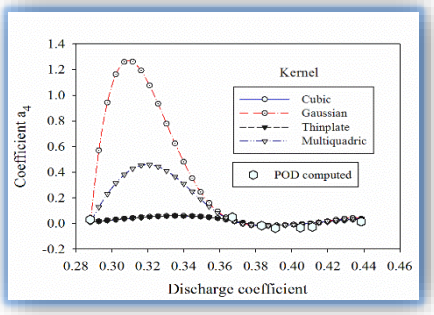

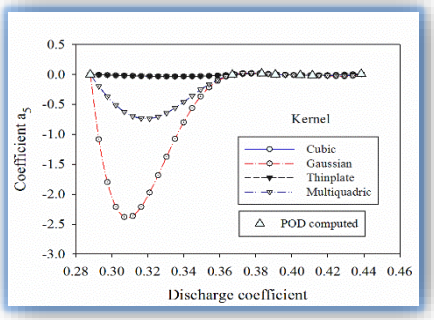

Figure 6. The RBF interpolated coefficients for axial perturbation vs. the POD computed coefficients

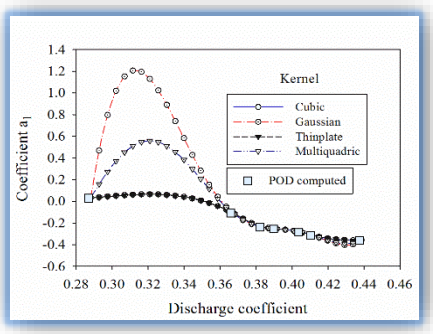

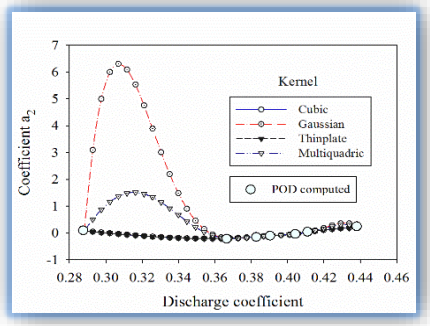

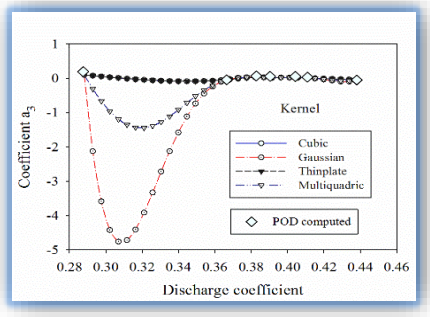

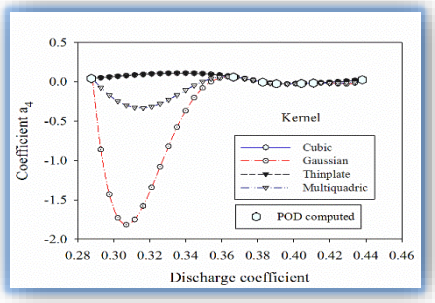

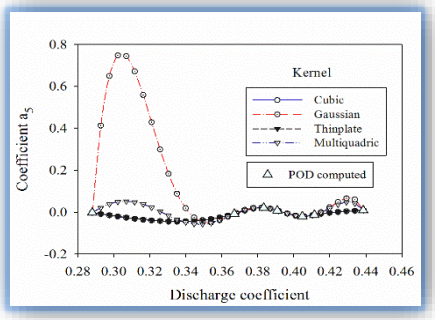

Figure 7. The RBF interpolated coefficients for circumferential perturbation vs. the POD computed coefficients

Specifically, the first five POD modes capture more than 99.92% of the total information contained in the original snapshot matrix, therefore we consider $p = 5$ the number of optimal POD basis functions retained for velocity fields estimation.

The orthonormal POD basis functions computed with the improved POD algorithm presented herein are depicted in Figure 5 for modal decomposition of the axial-circumferential velocity fields. The next figures illustrate the coefficients of the orthogonal decomposition interpolated using the method of RBF with the kernels listed in Table 1. Figure 6 presents the first five coefficients used for axial velocity decomposition and in Figure 7 the coefficients of the circumferential velocity are depicted, for the entire discharge window.

In addition to comparing coefficient profiles we compare the correlation coefficients of the reduced order model. The correlation coefficients defined below are used as additional metrics to evaluate the efficiency of the reduced order model

$$C^q = \frac{\left(\left\|v_{POD}(r;q)^H \cdot v(r;q)\right\|_2\right)^2}{\left\|v_{POD}(r;q)^H \cdot v_{POD}(r;q)\right\|_2 \left\|v(r;q)^H \cdot v(r;q)\right\|_2}, \quad (16)$$

where $v(r;q)$ represents the measured velocity profile at discharge q, $v_{POD}(r;q)$ is the estimated velocity profile obtained with the POD-RBF model, $\|\cdot\|_2$ stands for the Euclidean norm, $(\cdot)$ represents the Hermitian inner product and H denotes the conjugate transpose.

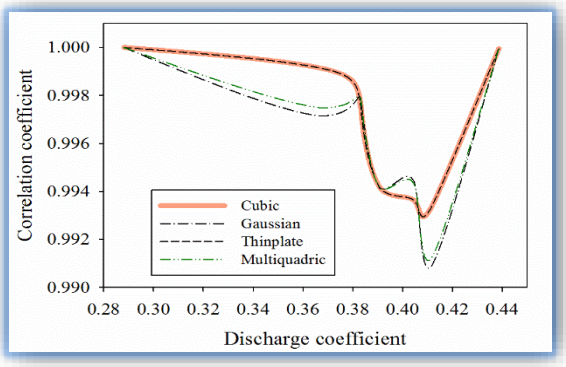

a.

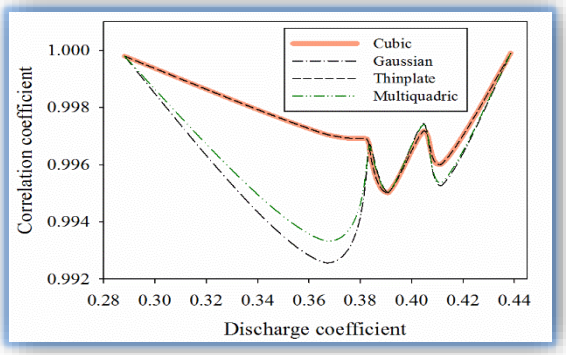

b.

Figure 8. Correlation coefficients for estimation of axial (a) and circumferential (b) perturbations of the velocity profiles using the POD-RBF model (present research).

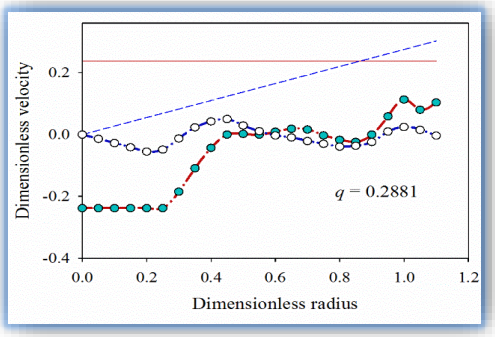

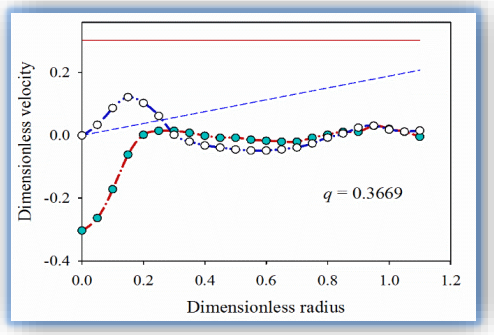

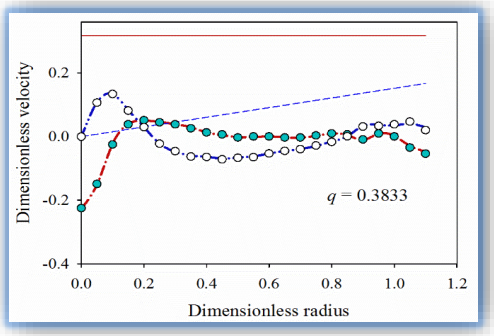

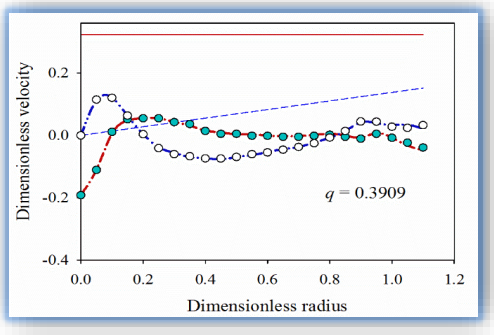

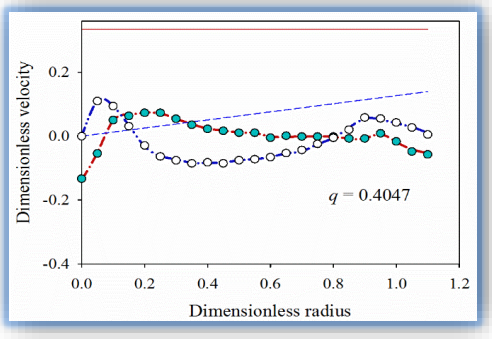

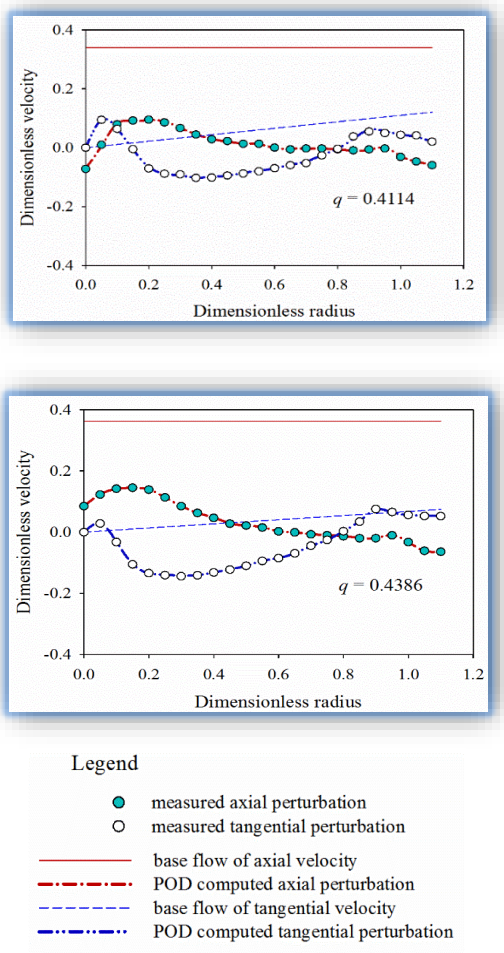

Figure 9. Velocity profiles estimated using the POD-RBF model (present research) in comparison with the experimentally measured profiles

A comparison of the correlation coefficients between the experimentally measured profiles and the reduced order models is provided in Figure 8. The values of the correlation coefficients are greater than 99% for axial and circumferential velocity profiles and confirm the validity of the reduced order model. Moreover, for the problem investigated in this paper, the most efficient kernels for RBF interpolation are both the cubic and the thinplate kernels.

In the following, we compare how the reduced order model assesses the velocity field in parallel with experimentally measured velocity profiles. The base flows of the axial and circumferential velocities have been computed respectively using the relations (5) and (7), whilst the velocity perturbations have been estimated employing the POD-RBF model developed in the paper, using the thinplate kernel. The numerical results are illustrated in Figure 9. Circles represent the measured velocity profiles for discharge coefficient q.

The perfectly match between the estimated velocity perturbations and the experimentally measured profiles confirms the efficiency of the reduced order model developed in this research.

SUMMARY AND CONCLUSIONS

In this paper we have proposed an algorithm for orthogonal decomposition of swirling flows in turbomachines. This framework is useful when a set of few experimentally measured velocity profiles are available and estimations of velocity profiles at intermediate discharge coefficients are needed.

We have implemented an algorithm based on Proper Orthogonal Decomposition in conjunction with Radial Basis Functions interpolation to obtain the reduced order model for estimation of the velocity perturbations. Key innovation for the model introduced in this paper resides in decomposition of the velocity field into a base flow part and a perturbation part, such that the resulting perturbation flow preserves a null discharge and a null moment of momentum flux, respectively. In consequence, the POD algorithm was applied to the perturbation flow quantity, for the axial and circumferential velocity filed, respectively. The proposed method allows the identification of the leading modes in the perturbed flow, modes that capture the most energy in the flow. The methodology presented herein offers an insight on the identification of the coherent structures in the perturbation flow. Once the leading coherent structures are identified, a hydrodynamic stability analysis of the perturbation flow can be performed. This is a topic that we will address carefully in our future work.

We have performed a rigorous error analysis of the reduced order model by computing the correlation coefficients when different kernels are employed for RBF interpolation. The values of the correlation coefficients greater than 99% for axial and circumferential velocity profiles, respectively, confirm the validity of the reduced order model.

By comparing the estimated reduced order solution with the experimentally measured profiles we emphasized an excellent behavior of the reduced order model.

Thus the methodology presented in this paper can be successfully applied not only to hydraulic turbines, but also for problems originating from different domains, where dynamics of the investigated phenomenon is strongly influenced by the system parameters.

ACKNOWLEDGEMENT

The first author acknowledges the partially support of strategic grant POSDRU/159/1.5/S/137070 (2014) of the Ministry of National Education, Romania, co-financed by the European Social Fund-–Investing in People, within the Sectorial Operational Program Human Resources Development 2007-2013. The second author was partially supported by a grant of the Romanian Ministry of Education and Scientific Research CNCS-UEFISCDI PN-II-ID-PCE-2012-4-0634

REFERENCES

[1.] M. Topor, D.A. Bistrian, Localization of the most amplified perturbation in a vortex rope located in Francis turbine at partial discharge, in: AIP Conf. Proc, Vol. 1493, 2012, pp. 1047–1053.

[2.] F. Frunzulica, A. Dumitrache, B. Suatean, Numerical investigations on dynamic stall control with passive elements, in: AIP Conf. Proc, Vol. 1648, 2015, pp. 500002, doi: 10.1063/1.4912700.

[3.] M. Osaci, Study about the possibility to control the superparamagnetism-superferromagnetism transition in magnetic nanoparticle systems, Journal of Magnetism and Magnetic Materials 343 (2013) 189-193.

[4.] D. Kosambi, Statistics in function space, Journal of the Indian Mathematical Society 7 (1943) 76–88.

[5.] M. Loeve, Probability Theory, Van Nostrand, 1955.
[6.] K. Karhunen, Zur Spektraltheorie Stochastischer Prozesse, 37, Ann. Acad. Sci. Fennicae, 1946.
[7.] A. Obukhov, Statistical description of continous fields, Trudy Geofizicheskogo Instituta, Akademiya Nauk SSSR 24 (1954) 3–42.
[8.] R. Stefanescu, A. Sandu, I.M. Navon, Comparison of POD reduced order strategies for the nonlinear 2D shallow water equations, International Journal for Numerical Methods in Fluids 76 (8) (2014) 497–521.
[9.] Z. Wang, I. Akhtar, J. Borggaard, T. Iliescu, Proper orthogonal decomposition closure models for turbulent flows: A numerical comparison, Computer Methods in Applied Mechanics and Engineering 237-240 (2012) 10–26.
[10.] A. Alekseev, I.M. Navon, Numerical control of two-dimensional shock waves in dual solution domain by instant temperature disturbances, International Journal for Numerical Methods in Fluids 71 (2013) 175–184.
[11.] R. Susan-Resiga, S. Muntean, F. Avellan, I. Anton, Mathematical modelling of swirling flow in hydraulic turbines for the full operating range, Applied Mathematical Modelling 35 (2011) 4759–4773.
[12.] R. Hardy, Multiquadric equations of topography and other irregular surfaces, Journal of Geophysical Research 76 (8) (1970) 1905–1915.
[13.] J. Duchon, Constructive Theory of Functions of Several Variables, Vol. Lecture Notes in Mathematics, Springer-Verlag, 1977, Ch. Splines minimizing rotation-invariant semi-norms in Sobolev spaces, pp. 85–100.
[14.] B. Fornberg, G. Wright, Stable computation of multiquadric interpolants for all values of the shape parameter, Computers and Mathematics with Applications 48 (2004) 853–867

ACTA Technica CORVINIENSIS
BULLETIN OF ENGINEERING
ISSN:2067-3809